

Measurement of the cross section for electron impact ionization of multi-electron ions

II. N^{2+} to N^{3+} and C^+ to C^{2+}

K. L. AITKEN, M. F. A. HARRISON and R. D. RUNDEL†

United Kingdom Atomic Energy Authority, Culham Laboratory, Abingdon, Berkshire

MS. received 22nd April 1971

Abstract. Absolute measurements have been made of the electron impact ionization cross sections for the reaction $N^{2+} + e \rightarrow N^{3+} + 2e$ and its isoelectronic partner $C^+ + e \rightarrow C^{2+} + 2e$. The technique of crossed beams was employed and, at incident electron energies in excess of about 100 eV, the cross section for N^{2+} can be expressed by

$$Q = \frac{567}{E} \lg \frac{E}{51.0} (10^{-17} \text{ cm}^2)$$

and that for C^+ by

$$Q = \frac{1060}{E} \lg \frac{E}{31.5} (10^{-17} \text{ cm}^2)$$

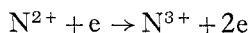
where E is in eV.

Measurements were extended to energies below threshold and the presence of metastable ions observed; their influence upon the measured cross sections is discussed.

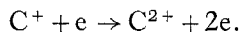
The present experimental data is compared with Coulomb-Born calculations by Moores, classical binary encounter calculations by Thomas and Garcia, and a semiempirical estimate by Lotz.

1. Introduction

The present paper reports absolute measurements of the electron impact ionization cross sections for the reaction



and its isoelectronic partner



The investigation is one of a series into multi-electron ions and was introduced in an earlier paper by Aitken and Harrison (1971) which will henceforth be referred to as Paper I. Previous experimental data for atomic nitrogen ions has been restricted to an absolute measurement of the cross section for $N^+ \rightarrow N^{2+}$ by Harrison *et al.* (1963) whose data is broadly substantiated by a relative measurement by Mahadevan (1970).

A. $N^{2+} + e \rightarrow N^{3+} + 2e$

2. Apparatus

The measurement was made using the crossed electron and ion beams apparatus described in Paper I and in previous papers. Some difficulty was encountered when

† Now at Department of Space Science, Rice University, Houston, Texas, 77001, USA.

extracting parent beams of multi-charged atomic ions from the ion source due to contamination by dissociation products from the much greater currents of molecular ions. Molecular ions which dissociate after being accelerated through the full ion extraction potential yield products of such an energy that they cannot be separated from the parent atomic ions by the field of the selector magnet. The product of such a dissociation has an effective mass to charge ratio $(m/q)_e$ given by

$$\left(\frac{m}{q}\right)_e = \left(\frac{q}{m}\right)_o \left(\frac{m}{q}\right)_d^2$$

where the subscripts o and d refer respectively to the original molecule and its dissociation product. Some N_2^+ ions dissociated to N^+ (with $(m/q)_e = 14/2$) which entered the N^{2+} ion collector, so contributing to the parent ion current. However, their presence could be detected by separating them from the parent beam using a vertical electrostatic field located at the exit of the collision region. In normal operation, N^{2+} ions were extracted from the source by a potential difference of 10 kV and the yield of N^{2+} to N_2^+ was optimized (at about 1 to 50) by maintaining a high potential (200 V) on the source anode and a low source pressure of N_2 gas at about 3 mtorr. The source discharge current was 100 mA and the instantaneous pulsed current of the N^{2+} beam was typically 3×10^{-9} A. Under these conditions the concentration of N^+ did not exceed 1% of the N^{2+} beam.

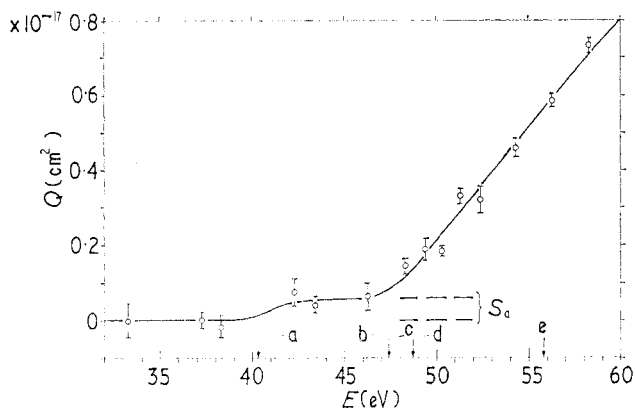


Figure 1. The measured ionization cross section of N^{2+} plotted against incident electron energy near to the threshold. The bars indicate 90% confidence limits of random errors. A smooth line passing through the points represents the probable behaviour of the measured cross section and includes the effect of energy spread of incident electrons. The arrows a to e represent the following thresholds: a, autoionization of the 4P metastable state; b, outer shell ionization of the 2P ground state; c, autoionization of the ground state; d, outer shell ionization of the 4P metastable state; e, inner shell ionization potential of the 2P ground state; S_a , the signal from autoionization of the 4P state at ground state threshold.

Greater difficulty was encountered from the dissociation of N_3^+ during the calibration of the electron multiplier using N^{3+} ions extracted from the source. An extraction potential of 6.66 kV was used to ensure the same ion velocity in both the calibrating and operating conditions. By using very low N_2 pressures in the source it was possible to reduce the yield of N_3^+ to about 10^{-10} A relative to N^{3+} calibration currents of 10^{-14} to 10^{-15} A. Under these conditions the N^{3+} beam contained up to

10% of N^+ arising from molecular dissociation and these ions were electrostatically deflected out of the beam so that the detector efficiency could be determined. The value obtained was $96.1 \pm 2.5\%$.

The conditions for the electron beam and methods of data acquisition were as described in Paper I. The maximum signal count rate was about $150 \text{ counts s}^{-1}$ falling by two orders near to the ionization threshold; the background of charged stripped N^{3+} ions was about $750 \text{ counts s}^{-1}$.

3. Metastable N^{2+} ions in the parent beam

As in previous measurements, the apparent cross section below the ionization threshold of N^{2+} was negative and displayed the $E^{-1/2}$ dependence upon electron

Table 1. Onset potentials for the electron impact ionization channels of C^+ and N^{2+}

SPC and N

Autoionization

$$\begin{array}{l}
 \left. \begin{array}{l} C^+ \\ N^{2+} \end{array} \right\} \begin{array}{l} \text{--- } 1s^2 2s 2p^2 \text{ } ^4P \\ \text{(metastable state)} \end{array} \quad \text{(excitation)} \quad \begin{array}{l} [19.4 \text{ eV}] \\ [41.0 \text{ eV}] \end{array} \\
 \\
 \left. \begin{array}{l} C^+ \\ N^{2+} \end{array} \right\} \begin{array}{l} \text{--- } 1s^2 2s^2 2p \text{ } ^2P \\ \text{(ground state)} \end{array} \quad \text{(excitation)} \quad \begin{array}{l} [24.8 \text{ eV}] \\ [48.1 \text{ eV}] \end{array}
 \end{array}
 \left. \begin{array}{l} \\ \\ \end{array} \right\} \begin{array}{l} \rightarrow C^+ \quad (1s^2 2s 2p 3d) \text{ } ^2F^{\circ}\dagger \\ \rightarrow N^{2+} \quad (1s^2 2s 2p 4d) \text{ } ^2F^{\circ}\dagger \end{array}$$

(Autoionization)

$$\begin{array}{l}
 C^{2+} \\
 N^{3+}
 \end{array}
 \left. \begin{array}{l} \\ \\ \end{array} \right\} (1s^2 2s^2) \text{ } ^1S + e$$

Outer shell ionization

$$\begin{array}{l}
 \left. \begin{array}{l} C^+ \\ N^{2+} \end{array} \right\} \begin{array}{l} \text{--- } (1s^2 2s^2 2p) \text{ } ^2P \\ \text{(ground state)} \end{array} \quad \begin{array}{l} [(24.4 \text{ eV})] \\ [(47.4 \text{ eV})] \end{array} \quad \begin{array}{l} \rightarrow C^{2+} \\ \rightarrow N^{3+} \end{array} \left. \begin{array}{l} \\ \\ \end{array} \right\} (1s^2 2s^2) \text{ } ^1S \\
 \\
 \left. \begin{array}{l} C^+ \\ N^{2+} \end{array} \right\} \begin{array}{l} \text{--- } (1s^2 2s 2p^2) \text{ } ^4P \\ \text{(metastable state)} \end{array} \quad \begin{array}{l} [(25.5 \text{ eV})] \\ [(48.7 \text{ eV})] \end{array} \quad \begin{array}{l} \rightarrow C^{2+} \\ \rightarrow N^{3+} \end{array} \left. \begin{array}{l} \\ \\ \end{array} \right\} (1s^2 2s 2p) \text{ } ^3P
 \end{array}$$

Inner shell ionization

$$\begin{array}{l}
 \left. \begin{array}{l} C^+ \\ N^{2+} \end{array} \right\} \begin{array}{l} \text{--- } (1s^2 2s^2 2p) \text{ } ^2P \\ \text{(ground state)} \end{array} \quad \begin{array}{l} [(30.9 \text{ eV})] \\ [(55.8 \text{ eV})] \end{array} \quad \begin{array}{l} \rightarrow C^{2+} \\ \rightarrow N^{3+} \end{array} \left. \begin{array}{l} \\ \\ \end{array} \right\} (1s^2 2s 2p) \text{ } ^3P \\
 \\
 \left. \begin{array}{l} C^+ \\ N^{2+} \end{array} \right\} \begin{array}{l} \text{--- } (1s^2 2s 2p^2) \text{ } ^4P \\ \text{(metastable state)} \end{array} \quad \begin{array}{l} [(36.1 \text{ eV})] \\ [(62.0 \text{ eV})] \end{array} \quad \begin{array}{l} \rightarrow C^{2+} \\ \rightarrow N^{3+} \end{array} \left. \begin{array}{l} \\ \\ \end{array} \right\} (1s^2 2p^2) \text{ } ^3P
 \end{array}$$

† Selection rules for autoionization demand ΔL and $\Delta S = 0$ for transitions into the continuum of the doublet terms $C^{2+} (^1S) + e_i$ and $N^{3+} (^1S) + e_i$. Hence these doubly excited states lie above the first ionization limit of C^+ and N^{2+} and are doublets of the form $(1s^2 2s 2p nl) ^2L$. The upper limits to (nl) are at the inner shell continuum (30.9 eV, C^+ ; 55.8 eV, N^{2+}) from the ground state and the outer shell continuum (25.5 eV, C^+ ; 48.7 eV, N^{2+}) from the metastable state. Excitation to the doublet states is allowed from the ground-state but disallowed from the metastable state. The autoionizing level quoted is the lowest listed in the spectroscopic tables of Moore (1949), but other unobserved levels may exist down to an excitation threshold of (19.1 eV, C^+ ; 40.3 eV, N^{2+}) for the metastable and (24.4 eV, C^+ ; 47.4 eV, N^{2+}) for the ground state.

energy which is characteristic of electron space charge deflection of the ion trajectories. Consequently the apparent cross section was corrected by an $E^{-1/2}$ term, determined from the signal below threshold, to yield the measured cross section which is shown plotted against incident electron energy up to 60 eV in figure 1. The correction amounted to 3.25% at the peak value of the measured cross section. Onset of ionization below the ^2P ground state threshold of N^{2+} is clearly demonstrated and arises from autoionization of the ^4P metastable state. Autoionization of multi-electron atoms has been discussed by Peach (1970) and onset potentials of the ionization channels of importance in the present measurement are given in table 1.

The autoionization cross sections exhibit the same energy dependence as excitation cross sections, which for ions are finite at threshold. This behaviour cannot be discerned from the experimental data due to the limited number of points, their statistical uncertainties, and the spread in electron energy. In the absence of a knowledge of the magnitude of the summated autoionization cross sections it is not possible to estimate the concentration of metastable ions. Neither is it possible to predict with certainty the energy dependence of their contributions to the measured cross section at energies above the ground state threshold of 47.4 eV. However, their contribution

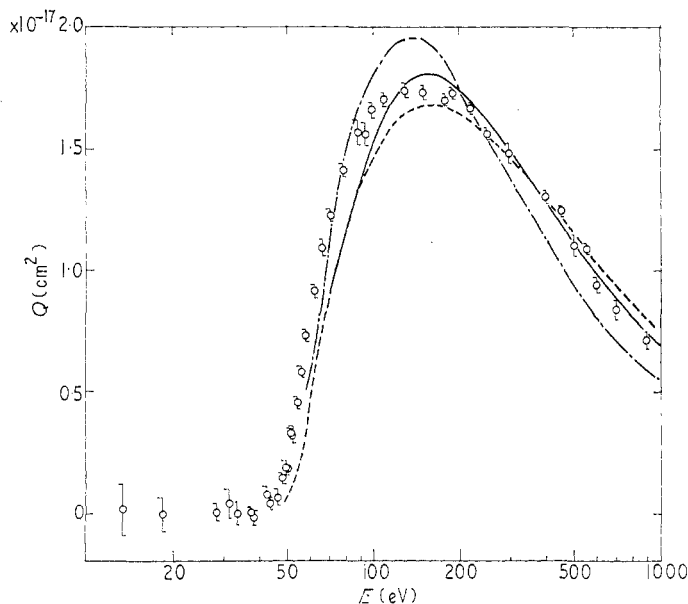


Figure 2. The measured ionization cross section of N^{2+} plotted against energy. The experimental points are shown with 90% confidence limits. Solid curve, Coulomb-Born calculation by Moores (1970); dashed curve, semiempirical result of Lotz (1968); broken curve, classical calculation from Thomas and Garcia (1969).

is not likely to exceed significantly that at the ground state threshold for the following reason: the excitation processes are disallowed and so at energies much in excess of 48.7 eV are likely to fall considerably faster than $\lg E/E$, which is the dependence of the measured ionization cross section at higher energies. Hence the magnitude of the autoionization signal at the ground state threshold (S_a in figure 1) can be taken as an upper limit of contributions from autoionization of $\text{N}^{2+}(^4\text{P})$. This upper limit is less than 3.5% of the peak value of the measured cross section.

Metastable ions also contribute to the measurement by inner and outer shell ionization and the semiempirical formulation of Lotz (1968) was used to calculate these cross sections. At energies in excess of the inner shell threshold of the metastable ion, the cross sections for the 4P and 2P states were found to differ by less than 2.0% indicating that, in this energy regime, the measured cross section is likely to differ from the ground state cross section mainly by the contribution from auto-ionization of the 4P state.

4. Results and discussion

The measured cross section is plotted as a function of incident electron energy in figure 2 and can be compared with the classical calculations of Thomas and Garcia (1969) and the results of D. L. Moores (1970 private communication) who used the Coulomb-Born approximation. The semiempirical determination of Lotz is also

Table 2

Mean incident electron energy† (eV)	Measured cross section Q_m (10^{-17} cm ²)	Random error‡ (± %)	Maximum possible¶ systematic error in Q_m (%)	
37.3	0.002	900	± 500	
38.3	-0.017	180	± 70	
42.3	0.075	48	+ 22	- 19
43.3	0.040	57	+ 33	- 31
46.3	0.064	58	+ 23	- 21
48.3	0.145	13	+ 15.0	- 12.5
49.3	0.188	16	+ 13.4	- 10.9
50.3	0.183	5	+ 13.4	- 10.9
51.3	0.330	6	+ 11.4	- 8.9
52.3	0.321	10	+ 11.4	- 8.9
54.3	0.457	6	+ 10.4	- 7.9
56.3	0.584	3	+ 9.7	- 7.2
58.3	0.732	3	+ 9.1	- 6.6
62.3	0.914	3	+ 8.9	- 6.4
66.3	1.093	3	+ 8.8	- 6.3
70.3	1.227	2	+ 8.6	- 6.1
78.3	1.411	2	+ 8.5	- 6.0
88.3	1.573	3	+ 8.5	- 6.0
93.3	1.561	3	+ 8.4	- 5.9
98.3	1.663	2	+ 8.4	- 5.9
108.3	1.708	2	+ 8.4	- 5.9
128.3	1.743	2	+ 8.4	- 5.9
148.3	1.734	2	+ 8.3	- 5.8
178.3	1.698	1	+ 8.3	- 5.8
188.3	1.730	2	+ 8.3	- 5.8
218.3	1.669	1	+ 8.3	- 5.8
248.3	1.561	2	+ 8.3	- 5.8
298.3	1.486	3	+ 8.3	- 5.8
398.3	1.303	1	+ 8.3	- 5.8
448.3	1.247	1	+ 8.3	- 5.8
498.3	1.104	4	+ 8.3	- 5.8
548.3	1.092	1	+ 8.3	- 5.8
598.3	0.942	3	+ 8.3	- 5.8
698.3	0.839	5	+ 8.3	- 5.8
898.3	0.711	5	+ 8.3	- 5.8

† ± 0.5 eV

‡ 90% confidence limits

¶ see table 3.

shown. Numerical data is listed in table 2 and the sources of systematic error appear in table 3.

Table 3

Possible source of systematic error	Maximum possible systematic error in the cross section (%)		
Measurement of signal (correction for counting system dead time)		± 0.1 (0.3)	
Calibration of electron multiplier		± 2.5 (1.5)	
Measurement of I	$+2.2$ (1.2)		-1.2 (0.2)
Measurement of J	$+1.25$		-0.25
Measurement of V		± 0.15	
Measurement of v		0	
Measurement of h		± 0.4	
Measurement of F		± 0.5	
Uncertainty of angle of beam intersection	$+0$		-0.5
$E^{-1/2}$ correction term		$\pm 0.4^\dagger$ (1.5 ‡)	
Contribution to I from extraneous ions in the parent beam ¶	$+1$		-0

Where the errors for C^+ differ from those for N^{2+} , the former are in brackets.

† At 100 eV and ‡ at 50 eV, reducing at higher energies, becomes the dominant error near threshold.

¶ N^+ in the N^{2+} beam.

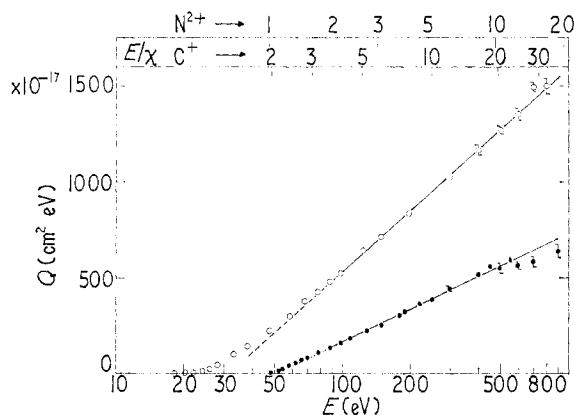


Figure 3. The product QE of the measured cross section Q and incident electron energy E plotted against $\lg E$. The error bars indicate 90% confidence limits where shown, otherwise they are within the circle diameters. Results for N^{2+} are shown by the solid circles and the linear relationship above 90 eV is given by equation (1). Results for C^+ are shown by open circles and the linear relationship above 100 eV is given by equation (2).

The Lotz formulation is in fair agreement with the measured cross section but classical calculation exhibits its customary imperfections at high energies although the peak value is more closely predicted than in the case of $O^+ \rightarrow O^{2+}$ (see Paper I). However, this agreement could be fortuitous because none of the calculations take

account of autoionization from the ground state ion. The same reservation must be applied to the Coulomb-Born results which exhibit unusually close agreement with the data around the peak of the cross section. Conversely the fact that the target ion is doubly charged would tend to enhance the validity of the Coulomb-Born approximation. There is no evidence within experimental limits of autoionization of the groundstate which would appear as a step in the slope of the measured cross section above the groundstate threshold.

The product QE is proportional to $\lg E$ over the range 90 to 600 eV (see figure 3) and so the cross section may be expressed by the relationship

$$Q = \frac{567}{E} \lg \frac{E}{51.0} (10^{-17} \text{ cm}^2) \quad (1)$$

where E is in electron volts. At the highest energies, the deviation of the experimental points is more likely due to experimental uncertainty than an indication of the slope flattening into the Bethe regime.

B. $C^+ + e \rightarrow C^{2+} + 2e$

5. Experimental approach

C^+ ions with an energy of 15 keV were produced from CO_2 gas fed to the ion source and a typical instantaneous value of the pulsed beam current was 3×10^{-8} A. The C^{2+} product ions were detected with an efficiency of 100 (+0, -1.5)% and the maximum signal was 4500 counts s^{-1} falling appreciably at electron energies close to threshold. The background from C^{2+} ions formed from the C^+ beam in charge stripping collisions was about 10 times greater than the maximum signal.

6. Results and discussion

The majority of measurements were made at an ion source anode potential of 75 V and possessed the same general characteristics as the previous data for N^{2+} . The signal at all energies below threshold is very slightly positive and exhibits an $E^{-1/2}$ dependence upon electron energy in accordance with the known effect of electron space charge modulation. Corrections for this effect are less than 1% at the peak value of the measured cross section. Some measurements were taken using a higher potential (200 V) applied to the ion source anode and exhibit a positive signal below threshold some 15 times greater than for the 75 V condition. At the same time, the background of C^{2+} charge stripped ions was also about 2.5 times greater. The cause of this larger background has not been positively identified but it is not due to the dissociation of C_2^{2+} which constituted less than 0.1% of the C^+ beam. The difference between the signals measured under the two conditions exhibits an $E^{-1/2}$ dependence at energies above and below threshold and is therefore identified as an electron space charge modulation of the larger background. Thus after correction using an $E^{-1/2}$ term the cross section data for the two conditions has been combined and the results are shown plotted against incident electron energies up to 40 eV in figure 4.

Autoionization of the 4P metastable state is clearly observable although a previous investigation (Redhead 1969), using mass spectrometry of trapped ions, did not reveal ionization below the ground state threshold. C^+ is isoelectronic with N^{2+} and has similar ionization channels which are listed in table 1, together with their threshold

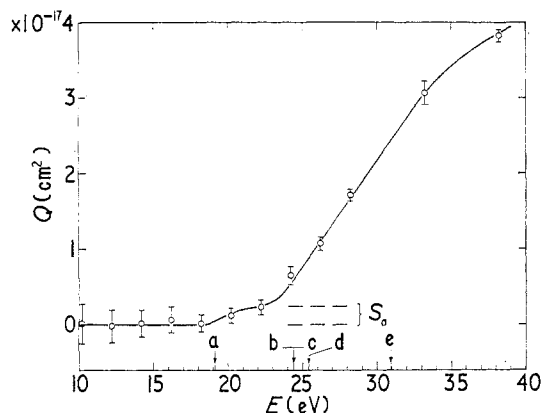


Figure 4. The measured cross section for ionization of C^+ by electron impact in the region near the threshold. For legend see figure 1.

energies. As in the case of N^{2+} , experimental limitations preclude identification of the finite step at threshold in the autoionization cross section for the 4P state; nor is it possible to estimate the concentration of these metastable ions in the 2P ground state beam. A comparison of the sum of the cross sections for inner and outer shell ionization of the metastable and ground state ions, calculated using the Lotz formulation,

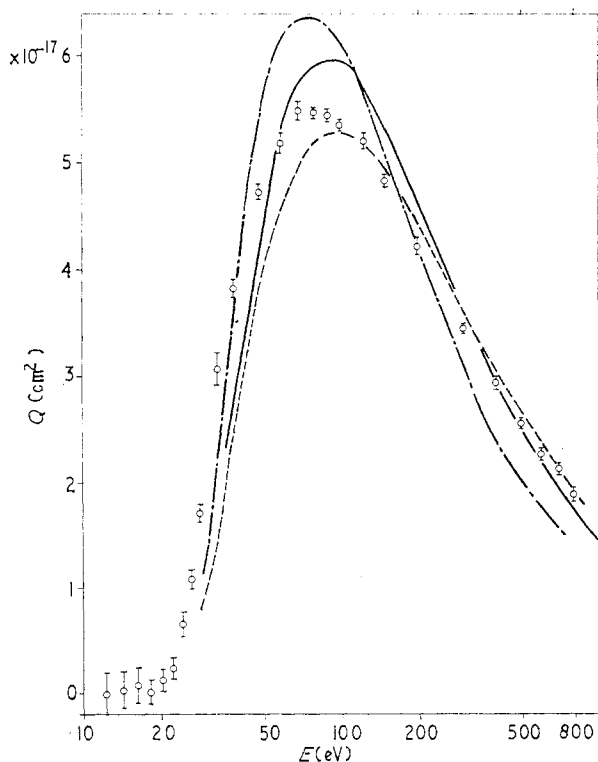


Figure 5. The cross section for the reaction $C^+ + e \rightarrow C^{2+} + 2e$ over the energy range 10 to 800 eV. For legend see figure 2.

indicates that at energies in excess of 50 eV the cross sections differ by less than 2%. Thus, as before, the upper limit of their contribution to the measured cross section is assumed to be that from autoionization at ground state threshold (S_a in figure 4) and is 4.5% of the peak value.

A significant feature in the present results is that an extrapolation of the linear onset of the measured cross section intercepts the contribution from autoionization of 4P ions at about 1 eV below groundstate threshold. This contrasts with the case of N^{2+} where no displacement in energy was observed. A possible explanation is that autoionization of ground state 2P ions gives rise to a significant step in the cross section at energies just above threshold. This hypothesis may be supported by the fact that autoionization of C^+ can arise from transition to the ($1s^2 2s 2p 3d$) states whereas the corresponding states for N^{2+} contain a 4d electron and may be less readily excited.

Numerical values of the measured cross section are given in table 4 together with random and systematic errors; the sources of the latter being given separately in table 3. A comparison with theory can be made by reference to figure 5 where the measured cross section is plotted together with various theoretical determinations. None of these calculations take into account autoionization of the groundstate. Nevertheless, the agreement exhibited by the Coulomb-Born calculation at peak values is less good than for the isoelectric case of N^{2+} but significantly better than for similarly charged O^+ (see Paper I). All three theoretical curves lie below the experimental one at energies up to twice times threshold suggesting that some contributions are not accounted for in the theory.

Table 4

Mean incident electron energy† (eV)	Measured cross section (10^{-17} cm^2)	Random error‡ ± %	Maximum possible systematic error¶ (%)	
18.2	0.01	1000	± 200	
20.2	0.121	82	± 80	
22.2	0.238	43	+ 58	- 56
24.2	0.655	18	+ 18.3	- 16.8
26.2	1.078	8	+ 12.3	- 10.8
28.2	1.714	4	+ 10.3	- 8.8
33.2	3.062	5	+ 7.9	- 6.4
38.2	3.82	2	+ 7.4	- 5.9
48.2	4.734	1	+ 6.8	- 5.3
58.2	5.187	2	+ 6.4	- 4.9
68.2	5.492	2	+ 6.3	- 4.9
78.2	5.47	1	+ 6.3	- 4.8
88.2	5.445	1	+ 6.2	- 4.7
98.2	5.349	1	+ 6.3	- 4.8
123.2	5.214	2	+ 6.3	- 4.8
148.2	4.84	1	+ 6.3	- 4.8
198.2	4.223	2	+ 5.8	- 4.3
298.2	3.442	1	+ 5.8	- 4.3
398.2	2.935	2	+ 5.8	- 4.3
498.2	2.552	1	+ 5.8	- 4.3
598.2	2.261	2	+ 5.8	- 4.3
698.2	2.126	2	+ 5.8	- 4.3
798.2	1.879	3	+ 5.8	- 4.3

† ± 0.5 eV.

‡ 90% confidence limits.

¶ see table 3.

The present results plotted in the form of QE against $\lg E$ in figure 3 show a linear relationship over the energy range from 100 eV up to the maximum of the experiment at 800 eV. The cross section may be expressed by

$$Q = \frac{1060}{E} \lg \frac{E}{31.5} (10^{-17} \text{ cm}^2) \quad (2)$$

where E is the incident electron energy in eV. Departure from linearity sets in at the relatively high energy of about 4χ and tends to support the view that in C^+ , at lower energies, autoionization contributions could be significant.

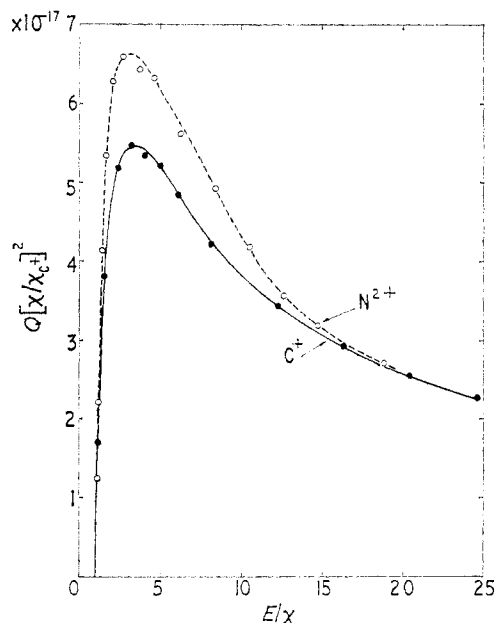


Figure 6. A comparison of the ionization cross section of C^+ (full line) with that of isoelectronic N^{2+} (broken line) scaled as $(\chi_{\text{N}^{2+}}/\chi_{\text{C}^+})^2$.

In figure 6 the measured cross section is plotted against energy expressed in units of the groundstate ionization potential χ . Also shown is data for the N^{2+} normalized by the classical scaling factor $(\chi_{\text{N}^{2+}}/\chi_{\text{C}^+})^2$. The results illustrate the applicability of the scaling law to this isoelectronic pair of ions at energies in excess of 15χ .

Acknowledgments

The authors wish to thank Dr D. L. Moores of University College, London, for providing us with his calculations before publication and helpful discussions on the autoionization effect, and in this respect we are also indebted to Dr C. Jordan and Dr A. H. Gabriel of the Astrophysical Research Unit, Culham Laboratory. We acknowledge the skilled assistance of G. H. Hirst and P. R. White of this laboratory.

References

- AITKEN, K. L., and HARRISON, M. F. A., Part I of this paper.
 HARRISON, M. F. A., DOLDER, K. T., and THONEMANN, P. C., 1963, *Proc. Phys. Soc.*, **82**, 368-71.

- LOTZ, W., 1968, *Z. Phys.*, **216**, 241–7.
- MAHADEVAN, P., 1970, *Abstr. 6th Int. Conf. on the Physics of Electronic and Atomic Collisions*, (Cambridge Mass: MIT Press) Pp 617–22.
- MOORE, C. E., 1949, *Atomic energy levels*, Vol. I, Nat. Bur. Stand. Circ. 467 (Washington: US Govt Printing Office).
- PEACH, G., 1970, *J. Phys. B: Atom. molec. Phys.*, **3**, 328–49.
- REDHEAD, P. A., 1969, *Can. J. Phys.*, **47**, 2449–57.
- THOMAS, B. K., and GARCIA, J. D., 1969, *Phys. Rev.*, **179**, 94–101.